Journal of the European Ceramic Society 19 (1999) 609–613

PII: S0955-2219(98)00232-5
0955-2219/99/$—see front matter

Mechanical Properties and Microstructure of Nano-SiC–Al_2O_3 Composites Densified by Spark Plasma Sintering

L. Gao,[a]* H. Z. Wang,[a] J. S. Hong,[a] H. Miyamoto,[b] K. Miyamoto,[b] Y. Nishikawa[b] and S. D. D. L. Torre[b]

[a]State Key Lab on High-Performance Ceramics and Superfine Microstructure, Shanghai Institute of Ceramics, Chinese Academy of Sciences, Shanghai 200050, Peoples Republic of China
[b]Technology Research Institute of Osaka Prefecture, Osaka 594-1157, Japan

(Received 5 July 1998; accepted 20 September 1998)

Abstract

Heterogeneous precipitation method has been used to produce 5 vol% SiC–Al_2O_3 powder, from aqueous suspension of nano-SiC, aqueous solution of aluminium chloride and ammonia. The resulting gel was calcined at 700°C. Nano-SiC–Al_2O_3 composites were densified using spark plasma sintering (SPS) process by heating to a sintering temperature at 1350, 1400, 1450, 1500 and 1550°C, at a heating rate of 600 °/min, with no holding time, and then fast cooling to 600°C within 2–3 min. High density composites could be achieved at lower sintering temperatures by SPS, as compared with that by hot-press sintering process. Bending strength of 5 vol% SiC–Al_2O_3 densified by SPS at 1450°C reached as high as 1000 MPa. Microstructure studies found that the nano-SiC particles were mainly located within the Al_2O_3 grains and the fracture mode of the nanocomposites was mainly transgranular fracture,

Keywords: nanocomposites, SiC, Al_2O_3, spark plasma sintering, sintering.

1 Introduction

Much attention has been focused on ceramic nanocomposites in which ceramic matrices are reinforced with submicrometer ceramic particles.[1] Several years ago, Niihara reported that the incorporation of small amounts (5–10 vol%) of nanoscale (0.3 μm diameter) SiC particles into Al_2O_3 matrix could significantly enhance the strength compared to pure Al_2O_3.[2] In their experiments, the strength increased from 350 MPa for Al_2O_3 to over 1 GPa for the 5 vol% SiC–Al_2O_3, and the toughness of Al_2O_3 was also shown to increase as a result of the SiC additions. Although other researchers have made efforts to repeat those results, the strength and toughness reported by Niihara are still difficult to reach so far. The dispersion of SiC homogeneously into Al_2O_3 matrix is found to be very important to fabricate the nanocomposites.

In our experiments, heterogeneous precipitation methods have been used to produce 5 vol% SIC–Al_2O_3 powder, from the aqueous solution of aluminium chloride mixed with the aqueous suspension of nano-SiC, followed by precipitation with ammonia. The resulting gel was calcined at 700°C. The nanoscale SiC particles (70 nm diameter) were randomly fine dispersed in γ-Al_2O_3,which transformed to α-Al_2O_3 during sintering process. The intragranular nanocomposites could be fabricated by this approach.

Spark plasma sintering is a new process that provides a means by which ceramic powder can be sintered very fast to fully dense. It is similar to hot-pressing which is carried out in a graphite die, but the heating is accomplished by spark discharges in voids between particles. generated by an instantaneous pulsed direct current applied through electrodes at the top and bottom punches of the graphite die. Due to these discharges, the particle surface is activated and purified, and a self-heat phenomenon is generated between the particles, thus the heat-transfer and mass-transfer can be completed instantaneously.[3–7] We used this new technique to sinter nano-SiC–Al_2O_3 composites and found that the sintering temperature for dense samples was at least 200°C lower than that by hot-press

*To whom correspondence should be addressed

sintering and the bending strength of the sample sintered at 1450°C reached as high as about 1 GPa due to the fine microstructures.

2 Experimental Procedure

2.1 Preparation of the powder

Nano-SiC particles (70 nm diameter), aluminium chloride ($AlCl_3 \cdot 6H_2O$) and ammonia were used as the three starting materials for preparing 5 vol% SiC–Al_2O_3 powder. The processing steps for the hetrogeneous precipitation method were outlined in Fig. 1. The aqueous suspension of nano-SiC was treated by the ultrasonic vibrating to break agglomerates and its pH was controlled between 9 and 10. Aqueous suspension of nano SiC was thoroughly stirred at room temperature, and then aqueous solution of aluminium chloride and ammonia were added to the suspension, with vigorous stirring until complete precipitation occurred, while pH value of the suspension was always kept between 9 and 10.

The resulting SiC–Al_2O_3 gel was washed with distilled water until chloride ion free (as tested by $AgNO_3$ solution) and then dried at 100°C. After grinding to pass through a 200 mesh sieve, the gel powder was calcined at 700°C for 2 h, followed by sieveing again through 200 mesh to give the final SiC–Al_2O_3 powder.

2.2 Spark plasma sintering

Spark plasma sintering (SPS) also known as pulsed electric current sintering (PECS)— was carried out in vaccum using Dr Sinter 1020 SPS apparatus (Sumitomo Coal Mining Co., Ltd., Japan), the schematic diagram of which is shown in Fig. 2. The prepared composite powder was carefully placed into a 20 mm diameter graphite die, and heated to the sintering temperatures at a heating rate of about 600°Cmin^{-1}. A pressure of approximately 40 MPa was applied from the beginning of sintering and was immediately relaxed as reached to the sintering temperature. There was no soaking time and the sintering sample was cooled to below 600°C within 2–3 min. The temperature was measured by means of an optical pyrometer focused on to the graphite die surface, which centred on the sintering sample. Sintered samples by SPS were approximately 20 mm in diameter and 5 mm thick.

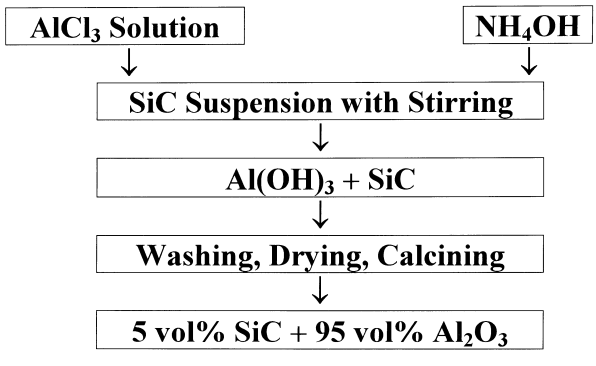

Fig. 1. Flow chart showing the fabrication of SiC–Al_2O_3 powder by the heterogeneous precipitation method.

2.3 Measurement of mechanical properties and observation of microstructure

Densities were measured by immersion in distilled water using Alchimedes principle. Sintered samples were cut and ground into rectangular bar specimens (4×3×18 mm). The bar specimens were carefully polished to a 600-grit SiC finish on one side and were levelled parallel to their lengths in order to eliminate edge flaws for bending strength testing. Bending strength was measured with Shimadzu AG-20KNG using three-point bending test with a span length of 10 mm and crosshead speed of 0·5 mm min^{-1}. Measurement of hardness and fracture toughness were made with Akashi AVK-C2 by indentation using a pyramidal indenter and applying a 10 kg load for 10 s.

TEM and SEM studies of microstructure were carried out using a Jeol 200CX Transmission Electron Microscope and a Philips XL20 Scanning Electron Microscope, respectively.

3 Results and Discussion

3.1 Dispersion of nano-SiC particles

It is critical to disperse nano-SiC particles homogeneously in Al_2O_3 matrix because the SiC particles are very fine and easy to aggregate. The relation between the zeta potential of SiC aqueous suspension and pH is shown in Fig. 3. The isoelectric point is shown near to pH4, and as the pH

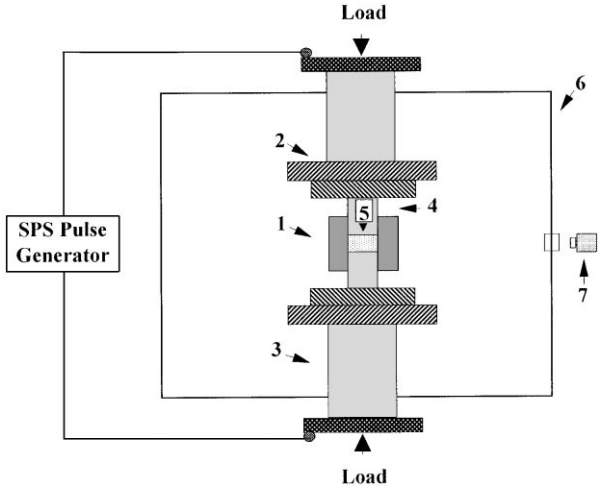

Fig. 2. Schematic diagram of the apparatus for spark plasma sintering (1, graphite die; 2, graphite plates; 3, ram; 4, graphite punch; 5, sample; 6, vacuum chamber; 7, optical pyrometer).

value of the suspension is far beyond this value, the SiC particles will repel each other due to the static electric force, making difficult for such particles to form agglomerate. As aqueous suspension of nano-SiC was treated by the ultrasonic vibrating to break agglomerates and its pH was controlled between 9 and 10, aqueous solution of aluminium chloride and ammonia were added to the suspension, well-dispersed nano-SiC–Al_2O_3 composite powder was obtained. TEM micrograph (Fig. 4) showed that the SiC particles were coated by γ-$A1_2O_3$ consisted of many fine particles which size was about 10 nm. The specific area of prepared 5 vol% SiC–Al_2O_3 powder is 150 m^2g^{-1}. Using such powder, it is possible to fabricate intragranular nanocomposites, because of the nano-SiC particles would be trapped in the Al_2O_3 grains as Al_2O_3 transformed from γ phase to α phase with grain growth during the sintering process.

3.2 Density and mechanical properties

The relative density of prepared composites versus the sintering temperature is shown in Fig. 5. It showed that nearly fully dense samples could be obtained by superfast SPS at 1450°C for SiC–Al_2O_3 composite powder, whereas for such powder sintered by hot-pressing, it needs a temperature of 1650°C at least and one hour soaking time.[1,2,8] The results proved that SPS is a potential method for fabricating nano-SiC-oxide composites at much lower temperature and within extreme short time.

Figure 6 showed the vickers hardness of the composites sintered by SPS versus the sintering temperature. The hardness tended to increase as the increasing sintering temperature rose to 1400°C, reaching to a hardness of 19 GPa, which was almost same for different sintering temperatures from 1400 to 1500°C and no significant difference from that of pure Al_2O_3. Figure 7 showed the bending strength of the composites superfast sintered by SPS versus the sintering temperature. The highest value achieved from the sample sintered at 1450°C was 980 MPa, which is much higher than that of monolithic Al_2O_3 ceramics (350 MPa). The addition of nano-SiC particles improved the microstructure of the composites and

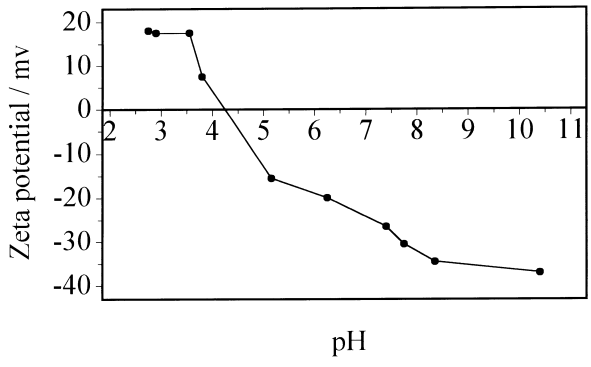

Fig. 3. The relation between the zeta potential of SiC aqueous suspension and pH value.

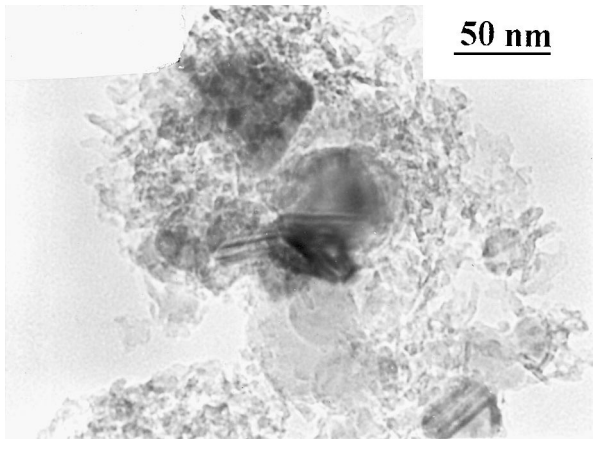

Fig. 4. TEM micrograph of SiC–Al_2O_3 Composite powder.

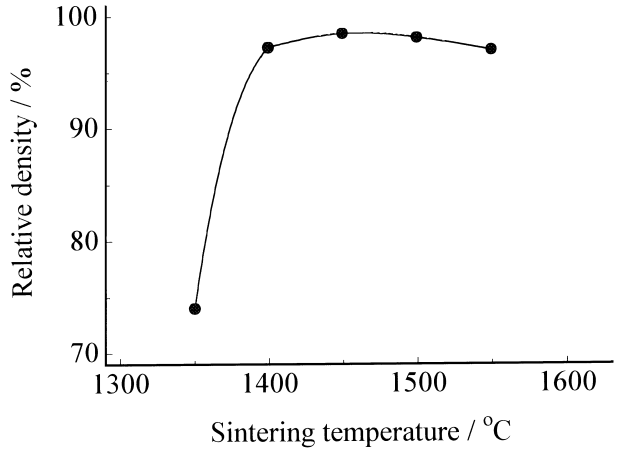

Fig. 5. Relative density versus sintering temperature for 5 vol% SiC–Al_2O_3 superfast sintered by SPS.

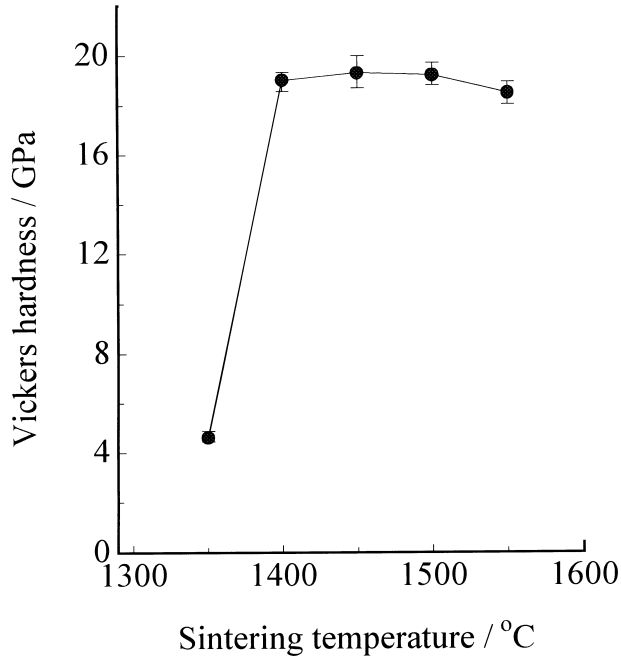

Fig. 6. Vickers hardness versus sintering temperature for 5 vol% SiC–Al_2O_3 superfast sintered by SPS.

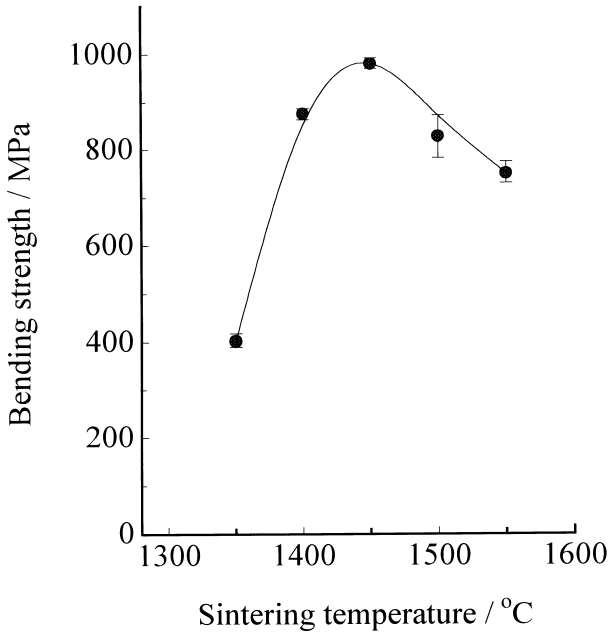

Fig. 7. Bending strength versus sintering temperature for 5 vol% SiC–Al_2O_3 superfast sintered by SPS.

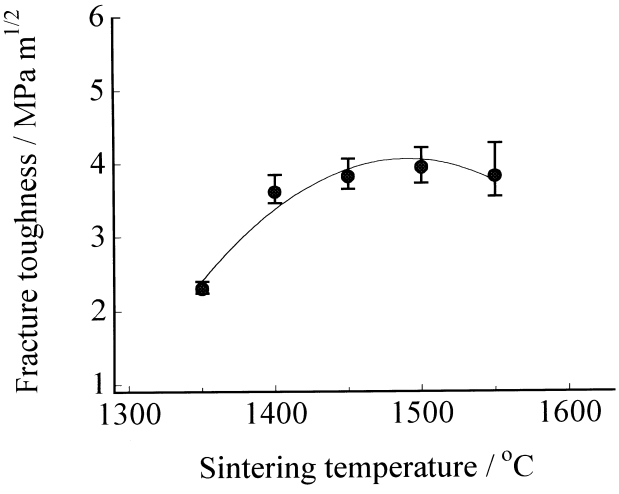

Fig. 8. Fracture toughness versus sintering temperature for 5 vol% SiC–Al_2O_3 superfast sintering by SPS.

enhanced the grain boundaries because of the residual stress resulted from the different thermal expansion coefficient of SiC and Al_2O_3. Figure 8 showed fracture toughness versus the sintering temperature. As compared with that of Al_2O_3 ceramics (3·5 MPa $m^{1/2}$), the fracture toughness values of the composites were also significantly improved.

3.3 Microstructure

Fig. 9 is a SEM micrograph of the fracture surface of SiC–Al_2O_3 nanocomposites showing the transgranular fracture mode, which benefited the improvement of the bending strength. Figure 10 is a TEM micrograph showing that nano-SiC particles were distributed throughout Al_2O_3 matrices. Most of nano-SiC particles were present inside

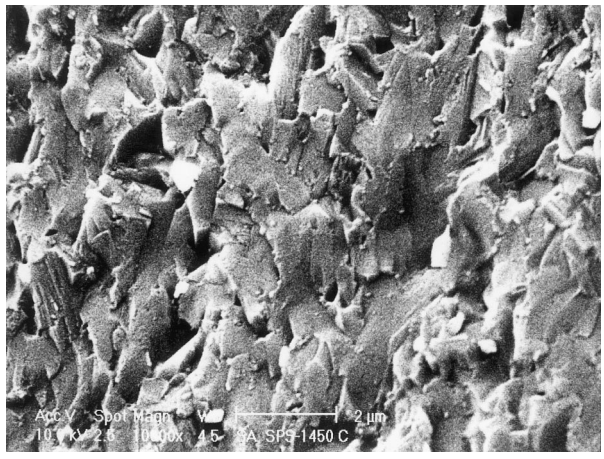

Fig. 9. SEM micrograph of fracture surface of SiC–Al_2O_3 nanocomposites.

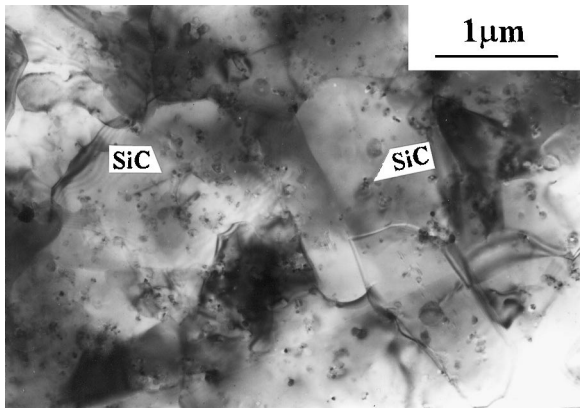

Fig. 10. TEM micrograph of SiC–Al_2O_3 nanocomposites.

Al_2O_3 grains, and only a few large particles were located at the boundaries or at the junctions of grains. It indicated that intragranular nanocomposites could be fabricated by this hetrogeneous precipitation method. For such kind of intragranular nanocomposites, the tensile residual stress would appear when the samples were cooled from the sintering temperature due to the expansion coefficient mismatch and most of SiC particles were located in Al_2O_3 grains. The tensile stress would weaken matrix grains and originate the transgranular fracture. As intragranular tensile stresses were transferred to the boundaries, it became compressive stresses and enhanced the boundary strength. SiC particles located on the boundaries inhibited the movement of boundaries and decreased the Al_2O_3 grain size. Thus, such a microstructure is very effective for improving the mechanical properties.

4 Conclusions

Nano-SiC–Al_2O_3 powder, in which the nano-SiC particles were coated by γ-Al_2O_3, was prepared by

the heterogenous precipitation method. To control pH value of aqueous suspension of nano-SiC between 9 and 10 during whole precipitation process is a key point for this purpose. It was successful that the powder was sintered to full dense by spark plasma sintering system at lower temperature and with no soaking time. The heating rate was as high as $600°C\,min^{-1}$ and the whole sintering process could be completed within a few minutes. The nano-SiC particles were mainly located within Al_2O_3 grains due to transformation of Al_2O_3 from γ- to α-phase. Bending strength of the intragranular nanocomposites was as high as 1 GPa, and its fracture mode was mainly transgranular fracture.

References

1. Zhao, J., Stearns, L., Harmer, M. P., Chan, H. M. and Miller, G. A., Mechanical behavior of alumina-silicon carbide nanocomposites. *J. Am. Ceram. Soc.*, 1993, **76**, 503–510.
2. Niihara, K., New design concept of structural ceramics-ceramic nanocomposites. *J. Ceram. Mc. Jpn.*, 1991, **99**, 974–982.
3. Tokita, M., Trends in advanced SPS spark plasma sintering system and technology. *J. Soc. Powder Tech. Jpn.*, 1993, **30**, 790–804.
4. Gao, L. and Miyamoto, H., Spark plasma sintering technology. *J. Inorg. Mater.*, 1997, **12**, 129–133.
5. Gao, L. Hong, J. S., Miyamoto, H. and Torre, S. D. D. L., Superfast densification of oxide ceramics by spark plasma sintering. *J. Inorg. Mater.*, 1998, **13**, 18–22.
6. Perera, D. S. , Tokita, M. and Moricca, S., Comparative study of fabrication Of Si_3N_4/SiC composites by spark plasma sintering and hot isostatic pressing. *J. Euro. Ceram. Soc.*, 1998, **18**, 401–404.
7. Tarnari, N., Tanaka, T. Tanaka, K., Kondoh, I. Kawahara, M. and Tokita, M., Effect of spark plasma sintering on densification and mechanical properties of silicon carbide. *J. Ceram. Soc. Jpn.*, 1998, **103**, 740–742.
8. Piciacchio, A., Lee, S. and Messing, G. L., Processing and microstructure development in alumina-silicon carbide intragranular particulate composites. *J. Am. Ceram. Soc.*, 1994, **77**, 2157–2164.